

# Patterns in 500 hPa geopotential height associated with temporal clusters of tropical cyclone tornadoes

Todd W. Moore<sup>a\*</sup> and Richard W. Dixon<sup>b</sup>

<sup>a</sup> Department of Geography and Environmental Planning, Towson University, Towson, MD, USA

<sup>b</sup> Department of Geography, Texas State University-San Marcos, San Marcos, TX, USA

**ABSTRACT:** Tropical cyclones are known to produce tornadoes, but the total number of tornadoes a tropical cyclone will produce, or the rate at which it will produce tornadoes throughout its lifespan, is not well understood. To understand better the link between the large-scale environment in which a tropical cyclone is located and tornado production, this study analyses and classifies 500 hPa geopotential height plots that correspond to temporal clusters of tornadoes. The primary 500 hPa patterns identified in this study represent various stages of interaction with the mid-latitude westerlies that a tropical cyclone may experience as it tracks from the tropics and subtropics to the mid-latitudes. Statistical analysis of the number of tornadoes *per* cluster suggests that tropical cyclones produce more tornadoes when they begin to interact with, or become embedded within, the mid-latitude westerlies.

**KEY WORDS** synoptic climatology; synoptic patterns; tropical cyclones; tornadoes

Received 5 August 2013; Revised 11 January 2014; Accepted 21 January 2014

## 1. Introduction

Tropical cyclones (TCs) often produce tornadoes (TCTORs) over a period of several days about their landfall, or as they track along the coastline without making landfall. The number of TCTORs a TC produces over its life span is quite variable, with some producing none or only a few, whereas others produce more than 100 (Novlan and Gray, 1974; Verbout *et al.*, 2007; Moore and Dixon, 2011). The rate at which a single TC produces TCTORs throughout its lifespan also varies (Moore and Dixon, 2013). Additional research into the environment in which TCTORs occur is needed to gain a better understanding of TCTOR variability, both between TCs and within a single TC's life span. This insight may help forecasters issue more accurate TCTOR outlooks and warnings and, in turn, mitigate human casualties.

Previous studies have investigated the environment in which TCTORs occur at various spatial scales. At the meso- and storm scales, studies have employed an approach similar to the ingredients-based approach used for mid-latitude supercell tornadoes (Doswell, 1987; Johns and Doswell, 1992; Doswell *et al.*, 1993) by focusing on the concurrence of vertical wind shear, instability, and lifting mechanisms within the TC environment (McCaul, 1991; McCaul and Weisman, 1996; Edwards and Pietrycha, 2006; Edwards, 2008, 2010a; Baker *et al.*, 2009; Edwards, 2012); moisture often is not a focus given the abundance of low-level moisture in the TC environment (Edwards, 2012). These studies have shown, generally, that TCTORs are most common in high-shear environments, often with only weak to moderate instability and a lifting mechanism such as a baroclinic zone.

At the synoptic scale, studies have employed a pattern recognition approach to examine links between TCTORs and the

larger-scale environment in which a TC is located. These studies have reported patterns in multiple atmospheric fields, including relative humidity at various geopotential height surfaces (Curtis, 2004; Cohen, 2010), surface pressure, temperature, and winds (Edwards and Pietrycha, 2006), and various geopotential height surfaces (Verbout *et al.*, 2007; Cohen, 2010). Both Curtis (2004) and Cohen (2010) identified similar mid-level relative humidity patterns associated with tornadic TCs. Curtis (2004) reported two patterns: one in which a region of dry air to the northwest of a TC's outer circulation splits to the northwest and northeast as the TC approaches, and another where a region of dry air intrudes into the TC environment, often from the east. Similarly, the composite for substantially tornadic TCs produced by Cohen (2010) shows a region of dry air cyclonically enveloping the TC and entraining into its eastern portion. Cohen (2010) found that substantially tornadic TCs, especially those in the southeastern United States, often are accompanied by an enhanced upper-level (200 hPa) jet streak to the north. When examining surface pressure, temperature, and winds, Edwards and Pietrycha (2006) found that TCTORs often occur proximate to baroclinic zones within the TC environment.

Two studies examined 500 hPa geopotential height composites associated with TCTORs (Verbout *et al.*, 2007; Cohen, 2010). Verbout *et al.* (2007) found that 500 hPa geopotential height composites distinguish between landfalling TCs in Texas that produced TCTOR outbreaks and those that do not produce outbreaks. TCTOR outbreaks in Texas were associated with a mid-latitude trough over the North Central United States to the north–northwest of the TC feature. The mid-latitude trough was shifted to the west in the non-outbreak composite and a ridge was positioned over the North Central United States. Similarly, Cohen (2010) produced 500 hPa geopotential height composites for substantial and non-substantial TCTOR-producing TCs along the Gulf Coastline of the United States, which he separated into western, central and eastern regions to minimize the

\* Correspondence: T. W. Moore, Department of Geography and Environmental Planning, Towson University, Towson, MD 21252, USA. E-mail: tmoore@towson.edu

smoothing induced by compositing. His composites for substantial TCTOR producers in all three regions show a trough situated generally over the western United States, farther from the TC feature than the trough in the Verboort *et al.* (2007) outbreak composite. Although Cohen (2010) did not report any substantial differences in trough/ridge patterns between the substantial and non-substantial TCTOR producers, he did report a deeper 500 hPa geopotential height depression in association with those TCs that produced a substantial number of TCTORS.

Previous studies have also noted the importance of mid-latitude environmental wind shear to the occurrence of TCTORS. McCaul (1991) for example, proposed that, as a TC is introduced into the mid-latitude westerlies (hereafter referred to as the westerlies), it encounters across-TC shear that may enhance potentially localized shear and helicity, and thus TCTOR development, especially within the right-front quadrant of the TC environment. Verboort *et al.* (2007) reported that nearly all of the TCs in their study that produced TCTOR outbreaks recurved northeastward over the southern or eastern United States, whereas those TCs that did not produce an outbreak maintained a westward heading or recurved over or off the eastern United States, thus placing the favourable right-front quadrant offshore. Similarly, other studies (Smith 1965; Hill *et al.*, 1966; Novlan and Gray, 1974; Moore and Dixon, 2011) have reported that recurring TCs are more likely to produce larger numbers of TCTORS than those that do not recurve. Verboort *et al.* (2007) also reported that North Atlantic TCs are more likely to produce a relatively large number of TCTORS during El Niño seasons when anomalously strong upper-tropospheric westerlies and environmental wind shear are located above the western Atlantic and Caribbean than during neutral and La Niña seasons when shear is weakened in this region; it should be noted, however, that this relationship was not statistically significant.

Further analysis of the link between TCs, their location relative to the westerlies, and TCTOR production is needed to complement Verboort *et al.*'s (2007) and Cohen's (2010) 500 hPa composite analyses and to assess further the importance of the westerlies to TCTOR production as noted by McCaul (1991) and Verboort *et al.* (2007). This study examines the 500 hPa geopotential height fields in which TCs were located when they produced a temporal cluster of TCTORS in the United States over the period 1995–2010. Particular attention is given to the location of the TCs relative to the westerlies during the analysis and classification of the 500 hPa geopotential height plots.

## 2. Data and methods

TCTOR clusters were identified from the TCTOR dataset, which includes information from the Storm Prediction Center's one-tornado database (ONETOR) and the National Hurricane Center's Atlantic hurricane database (HURDAT) (Edwards, 2010a, 2010b). The TCTORS in this dataset were verified to have been located within the cyclonic envelope of their parent TC using surface weather maps, upper air maps, and archived satellite and radar imagery (Edwards, 2010a). At the time of data collection, this dataset included information for TCTORS produced by Gulf Coast and East Coast landfalling TCs (including tropical depressions, tropical storms, hurricanes, and their extratropical and remnant phases) over the period 1995–2010. Sixty-five TCs produced a reported 1163 TCTORS over this period.

The 500 hPa geopotential height plots from the National Centers for Environmental Prediction–North American Regional Reanalysis (NCEP–NARR) project (Mesinger *et al.*, 2006) were used in the synoptic analysis and classification. NCEP–NARR

plots are gridded at a spatial resolution of (32 km<sup>2</sup>) and are available every 3 h beginning at 0000 UTC. The 500 hPa plots and composites shown in this study were obtained from the Physical Science Division of the National Oceanic and Atmospheric Administration's Earth System Research Laboratory and are plotted at a 50 m interval between 5000 and 6000 m (NOAA, 2013).

The environment-to-circulation approach (Yarnal, 1993) to synoptic classification was employed in this study; thus, only synoptic plots corresponding to TCTOR clusters were analysed and classified. Temporal clusters were defined as three or more TCTORS in a 6 h period, where the 6 h periods are centred about 0000, 0600, 1200 and 1800 UTC. This definition identifies relatively short time periods when TCs are producing a relatively large number of TCTORS rather than an isolated one or two. The 6 h periods were centred about 0000, 0600, 1200 and 1800 UTC (hours when NCEP–NARR plots are available) in order to ensure that the TCTORS in a particular cluster and the synoptic plots used to represent the 500 hPa environment during that cluster were synchronized temporally. This way, all TCTORS in a particular cluster occur within 3 h of their corresponding synoptic plot. This definition also captures more variability in the observed synoptic patterns associated with TCTORS than would be captured by the compositing technique or by the use of a longer temporal window.

Once the TCTOR clusters were identified, the 500 hPa geopotential height plots corresponding to the central hour of each cluster were collected. For example, TC Hermine (2010) produced eight TCTORS between 2100 and 0259 UTC on 8–9 September 2010. The 500 hPa geopotential height plot for 0000 UTC on 9 September 2010 was used to represent the environment in which this cluster occurred.

The 500 hPa geopotential height plots were classified manually using a TC-relative framework. Two TCs that appear as closed shortwave troughs at the 500 hPa level (Figure 1) can be considered as an example. While the overall map pattern of these events are dissimilar (i.e. the absolute locations of the synoptic features and the tilt of the trough axes are different), they would be classified the same using a TC-relative framework because both represent similar stages of interaction between a TC and the westerlies and, furthermore, each TC would likely be encountering similar synoptic-scale forcing.

## 3. Results

One hundred and thirty-three temporal clusters were identified in the TCTOR dataset. The clusters were classified and analysed by synoptic pattern to determine if TCs produce more TCTORS during certain stages of westerly interaction. Moore and Dixon (2013) provide a statistical description of the number of tornadoes *per* cluster for all 133 TCTOR clusters.

### 3.1. Description of 500 hPa geopotential height patterns

Three primary patterns were identified: (1) TCs that were isolated from the westerlies; (2) TCs that were beginning to interact with the westerlies; (3) TCs that were embedded within the westerlies as shortwave troughs. These patterns represent different stages of interaction with the westerlies that a TC may experience as it tracks from the tropics or subtropics to the mid-latitudes. Six sub-patterns, two within each primary pattern, also were identified based on the TCs' circulation at the 500 hPa level (i.e. closed or not) (Figure 2).

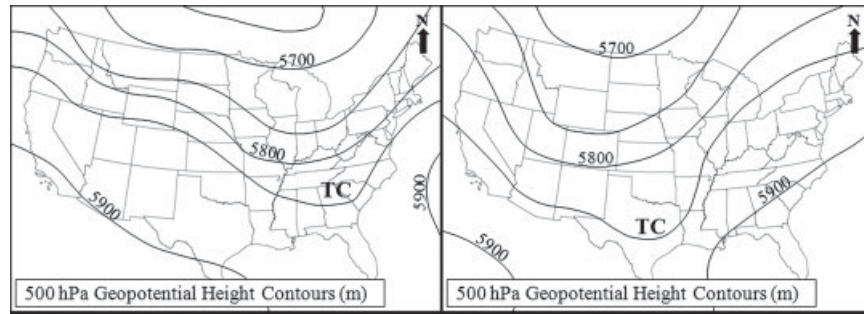


Figure 1. Simplified illustration of 500 hPa geopotential height fields associated with two tropical cyclones (TCs). In the TC-relative framework used in this study, these TCs are classified the same because both TCs are in similar stages of interaction with the westerlies (i.e. they are embedded within the southern-most circumpolar isoheight as shortwave troughs).

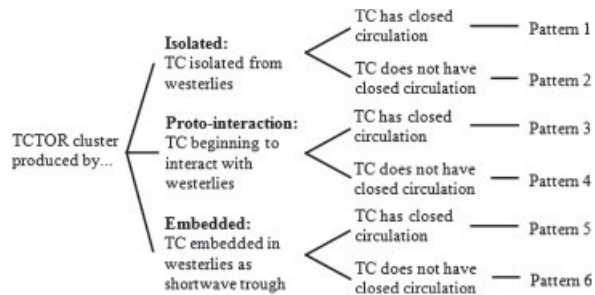


Figure 2. Classification tree (TCTOR, tropical cyclone tornado; TC, tropical cyclone).

Pattern 1 and 2 clusters were produced by TCs that were isolated from the westerlies (Figures 3(a) and (b)). These TCs were located typically to the south, or in the southern portion of, a well-defined subtropical ridge, placing a region of higher geopotential heights and unorganized flow between the TC circulation and the organized westerly flow to the north. These two patterns are differentiated by TC circulation at the 500 hPa level [i.e. closed (Pattern 1; Figure 3(a)) or open (Pattern 2; Figure 3(b))].

Pattern 3 and 4 clusters were produced by TCs that, like Patterns 1 and 2, were not embedded within the westerlies but, unlike Patterns 1 and 2, they were not separated from the organized westerly flow by a region of higher geopotential heights. These TCs were deemed to have begun interacting with the westerlies, but were not embedded because they were not encompassed by the southern-most circumpolar isoheight (Figures 4(a) and (b)). Patterns 3 and 4 are differentiated by TC circulation at the 500 hPa level (Pattern 3 = closed, Pattern 4 = open (Figures 4(a) and (b), respectively)).

Pattern 5 and 6 clusters were produced by TCs that were embedded within the westerlies (Figures 5(a) and (b)). These TCs were determined to be embedded within the westerlies because they were encompassed by the southern-most circumpolar isoheight (typically 5800 or 5850 m), giving them the appearance of shortwave troughs. The TCs that produced Pattern 5 clusters had a closed isoheight, giving them the appearance of a closed shortwave trough (Figure 5(a)), whereas those that produced Pattern 6 clusters did not have a closed isoheight and appeared as an open shortwave trough (Figure 5(b)).

### 3.2. Cluster frequency and severity

Eighty-three percent of the TCTOR clusters were produced by TCs that were beginning to interact with or were embedded

within the westerlies. Out of the three primary patterns, embedded TCs were responsible for the modal frequency of 62 clusters. Ninety-one percent of the TCTORs that occurred in a cluster were produced by proto-interaction and embedded TCs. Clusters produced by the proto-interaction and embedded TCs also were typically more severe than those produced by isolated TCs, as indicated by their mean and median metrics (Table 1). TCs that were beginning to interact with or embedded within the westerlies produced the majority of the most prolific clusters (Figure 6); the top 10 TCTOR-producing clusters ( $\geq 16$  TCTORs) were associated with proto-interaction or embedded TCs. The abundance and magnitude of these extreme clusters give the proto-interaction and embedded TCs relatively large cluster variability metrics (i.e. standard deviation and inter-quartile range; Table 1).

The result of the Kruskal–Wallis test shows that the mean ranks of the primary pattern pairs are not statistically similar (Table 2). *Post hoc* Mann–Whitney *U* tests with Bonferroni adjustment reveal that significant differences in mean ranks exist between the isolated and proto-interaction TCs and between the isolated and embedded TCs; proto-interaction and embedded TCs were not significantly different (Table 3). This is evident when examining the relationship between the mean ranks. The mean ranks for the proto-interaction and embedded TCs are nearly double that of the isolated TCs but are almost identical (Tables 2 and 3). One-tailed Mann–Whitney *U* tests verify that the mean ranks for both the proto-interaction and embedded TCs are significantly larger than that of the isolated TCs, which implies that TCTOR clusters produced by proto-interaction and embedded TCs tend to comprise more TCTORs than clusters produced by isolated TCs. The absence of a significant difference between the proto-interaction and embedded pattern clusters suggests that these two patterns may have similar synoptic-scale forcing provided by the westerlies.

Table 1 illustrates that TCs with closed circulation at the 500 hPa level typically produce larger TCTOR clusters. For example, the mean and median metrics are greater with Pattern 5 (closed isoheight) than with Pattern 6 (no closed isoheight). This is consistent with Cohen's (2010) 500 hPa geopotential height composites, which depict a closed isoheight in association with substantially tornadic TCs, whereas non-substantially tornadic TCs did not have a closed isoheight. These results support previous climatologies (e.g. Verbout *et al.*, 2007; Belanger *et al.*, 2009; Moore and Dixon, 2011) which reported that larger and stronger TCs have produced generally larger numbers of TCTORs.

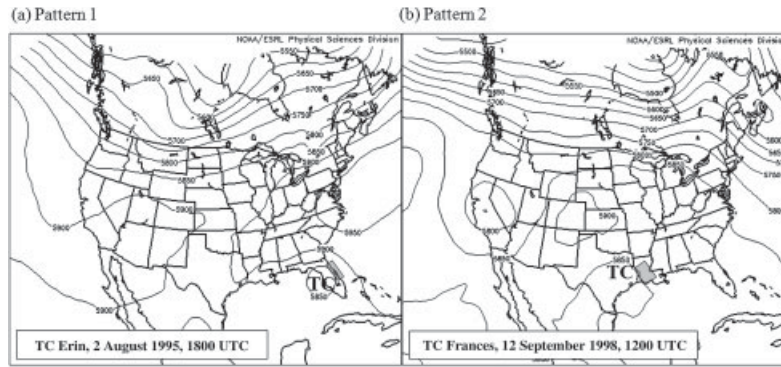


Figure 3. Plots of 500 hPa geopotential height (m) showing tropical cyclones (TCs) that were isolated from the westerlies when they produced a temporal cluster of tropical cyclone tornadoes (TCTORs). The grey polygon represents the general location of the cluster. Plots obtained from NOAA (2013).

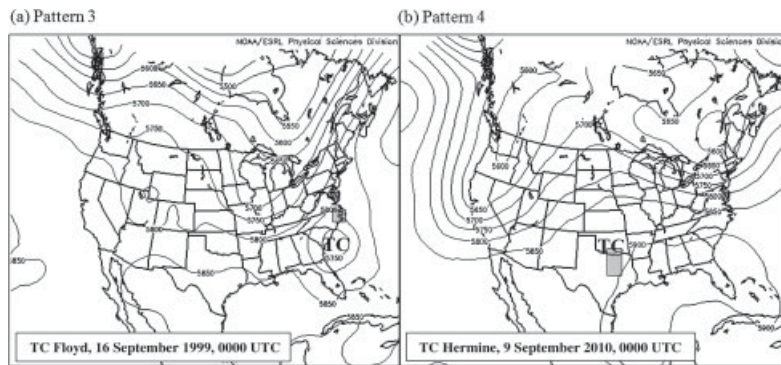


Figure 4. Plots of 500 hPa geopotential height (m) showing tropical cyclones (TCs) that were beginning to interact with the westerlies when they produced a temporal cluster of tropical cyclone tornadoes (TCTORs). The grey polygon represents the general location of the cluster. Plots obtained from NOAA (2013).

### 3.3. Spatial and temporal distributions

The TCTOR clusters occurred primarily in coastal states along the Gulf of Mexico and Atlantic Ocean (Figure 7). In the absence of shear associated with the westerlies and the jet stream, clusters produced by isolated TCs likely depend on low-level shear produced by mechanical friction during water-to-land transition as proposed by Gentry (1983). Dependence on friction-induced shear is a likely reason for the spatial clustering along the Gulf and East Coastlines of TCTORs produced by isolated TCs (Figure 7). TCs interacting with the westerlies are less dependent

on friction-induced shear because of the westerly shear they encounter, which allows them to produce TCTORs not only along the coastline but also further inland (Figure 7). Many of the TCTORs in the dense cluster throughout the Mid-Atlantic region were produced by TCs Frances (2004), Ivan (2004), and Cindy (2005). While they are proximate to the East Coastline, they were produced >900 km inland of their parent TC's landfall location along the Gulf Coast. These clusters, therefore, were produced when their parent TCs were experiencing westerly shear and friction-induced shear as the easterly and southeasterly winds ahead of the TC centre moved ashore.

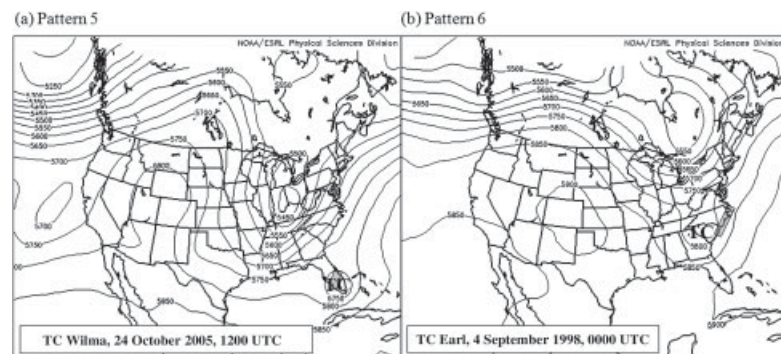


Figure 5. Plots of 500 hPa geopotential height (m) showing tropical cyclones (TCs) that were embedded in the westerlies as shortwave troughs when they produced temporal clusters of tropical cyclone tornadoes (TCTORs). The grey polygon represents the general location of the cluster. Plots obtained from NOAA (2013).

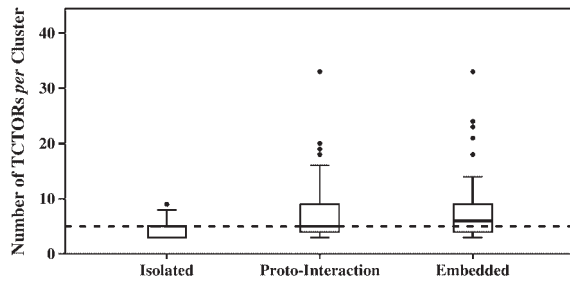


Figure 6. Boxplots showing the distribution of the number of tropical cyclone tornadoes (TCTORs) in clusters. The bottom and top of the boxes represent the 25<sup>th</sup> and 75<sup>th</sup> percentiles, respectively. The bold line within the boxes represents the median or 50<sup>th</sup> percentile. Whiskers extend to 1.5 times the inter-quartile range. Black dots beyond the whiskers represent statistical outliers. Dashed horizontal line represents the median number of TCTORs *per* cluster for all 133 clusters.

Table 1. TCTOR cluster statistics by primary- and sub-synoptic pattern.

Pattern	Number of clusters	Number of TCTORs	TCTOR cluster statistics		
			Mean	Median	Standard deviation
Isolated	22	93	4.2	3.0	1.8
Pattern 1	18	70	4.4	3.5	1.9
Pattern 2	4	13	3.3	3.0	0.5
Proto-interaction	49	367	7.5	5.0	6.0
Pattern 3	36	295	7.9	5.0	6.6
Pattern 4	13	82	6.3	4.0	4.0
Embedded	62	470	7.6	6.0	5.8
Pattern 5	22	235	10.7	9.0	7.4
Pattern 6	40	235	5.9	4.5	3.9

Table 2. Results of the Kruskal–Wallis test.<sup>a</sup>

Primary pattern	Number of clusters	Mean rank
Isolated	22	42.5
Proto-interaction	49	69.7
Embedded	62	73.5

Statistical significance was assessed at  $\alpha = 0.05$ .

<sup>a</sup> $\chi^2 = 11.2$ ,  $df = 2$ ,  $p = 0.004$ .

Overall, the clusters were most common in the 1800 and 0000 UTC periods, which span from late morning to late afternoon local time [0900–2059 Central Standard Time (CST)] when buoyant forcing is greatest (Figure 8(a)). Previous climatologies have shown similar diurnal signals in TCTOR counts (McCaul, 1991; Schultz and Cecil, 2009; Moore and Dixon, 2011; Edwards, 2012). By stratifying the clusters by primary pattern, this study also indicates that a disproportionately large number of clusters produced by TCs that are isolated from the westerlies occurred during the 0000 UTC period (1500–2059 CST), implying that these TCs may be more dependent on buoyant forcing for substantial TCTOR production than TCs that are beginning to interact with or embedded within the westerlies. Figure 8(a) also shows that a disproportionately large number of clusters produced by TCs that are interacting with the westerlies occurred during the 1200 UTC period (0300–0859 CST). This suggests that the larger-scale dynamic forcing likely to be present in these cases may favour substantial TCTOR production even in the absence of diurnal buoyant forcing.

Table 3. Results of the *post hoc* Mann–Whitney *U* tests.

Primary pattern	Number of clusters	Mean rank
Isolated <sup>a</sup>	22	26.2
Proto-interaction <sup>a</sup>	49	40.4
Isolated <sup>b</sup>	22	27.8
Embedded <sup>b</sup>	62	47.7
Proto-interaction <sup>c</sup>	49	54.3
Embedded <sup>c</sup>	62	57.3

According to the Bonferroni adjustment, each pattern-pair was assessed for statistical significance at  $\alpha = 0.017$ .

<sup>a</sup>Isolated *versus* proto-interaction: Mann–Whitney  $U = 323.0$ ,  $p = 0.006$ .

<sup>b</sup>Isolated *versus* embedded: Mann–Whitney  $U = 359.5$ ,  $p = 0.001$ .

<sup>c</sup>Proto-interaction *versus* embedded: Mann–Whitney  $U = 1437.0$ ,  $p = 0.623$ .

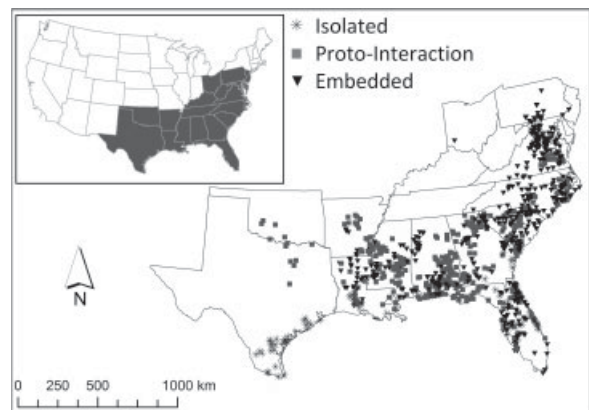


Figure 7. Spatial distribution of the tropical cyclone tornadoes (TCTORs) that occurred in a cluster stratified by primary pattern.

All clusters appeared to become more frequent from June to September as North Atlantic TC activity increased (Figure 8(b)), which is consistent with previous climatologies of TCTOR activity (Novlan and Gray, 1974; Moore and Dixon, 2011). The proto-interaction and embedded TCs have the greatest relative frequencies in September and October, respectively. This is likely associated with the expansion and strengthening of the westerly wind belt in the latter half of the North Atlantic hurricane season as the equator-to-pole temperature gradient increases (Harman, 1991).

#### 3.4. Tropical cyclones Ivan (2004), Frances (2004), and Rita (2005)

TCs Ivan (2004), Frances (2004), and Rita (2005) produced 118, 103 and 98 TCTORs respectively, making them the top three TCTOR producers in the United States over the 1995–2010 period. Composite plots illustrating the different primary patterns produced by each TC were created to illustrate further the 500 hPa geopotential height patterns identified in this study.

Ivan produced its first TCTOR at 1853 UTC on 15 September 2004 and its last at 0800 UTC on 18 September 2004, with eight clusters occurring over this roughly 3 day period. The first five clusters, during which 44 TCTORs occurred, were produced while Ivan was beginning to interact with the westerlies (Figure 9(a)). Three more clusters were produced as Ivan tracked northeastward and became embedded within the westerlies as a short wave trough (Figure 9(b)). Seventy-one TCTORs were produced throughout the northern part of Georgia, the Carolinas, the

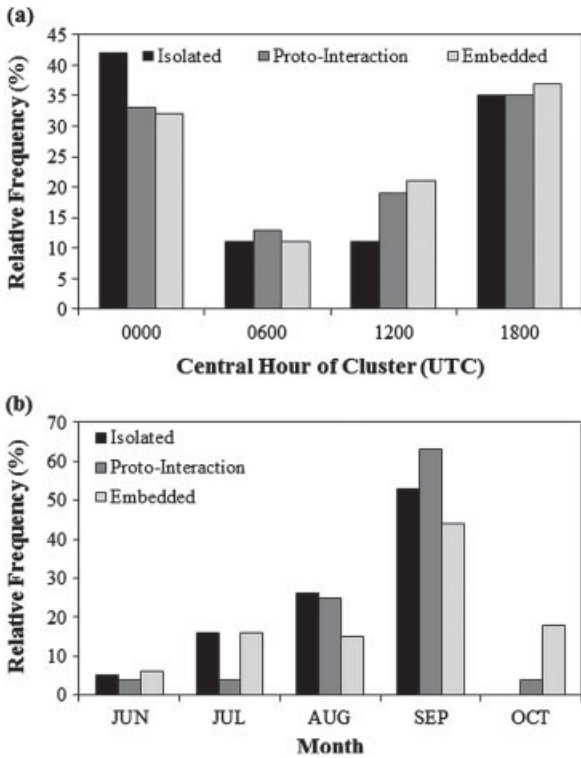


Figure 8. Diurnal (a) and monthly (b) relative frequency distribution of tropical cyclone tornado (TCTOR) clusters stratified by primary pattern.

Virginias, Maryland and Pennsylvania during this last embedded stage of Ivan’s lifespan.

Frances produced its first TCTOR at 1504 UTC on 5 September 2004 and its last at 0020 UTC on 9 September 2004. Twelve clusters were produced over this nearly 4 day period. The first four clusters were produced while Frances was located over the Florida peninsula to the south of a prominent mid-latitude ridge (Figure 10(a)). Only 15 TCTORs were produced during these clusters while Frances was isolated from the westerlies. The region of higher geopotential heights between the TC circulation and the mid-latitude trough over the Great Plains region diminished as Frances continued to track northwestward and the mid-latitude trough propagated eastward (Figure 10(b)). At this time, Frances became a proto-interaction TC and

produced four more clusters, including 31 TCTORs. Frances recurved and assumed a track towards the northeast under the influence of the westerlies and eventually became embedded as a shortwave trough (Figure 10(c)). Four more clusters, including 50 TCTORs, were produced during this last embedded stage.

Rita produced its first TCTOR at 1415 UTC on 24 September 2005 and its last at 1017 UTC on 25 September 2005, with six consecutive clusters over this period. Similar to Ivan’s clusters, all of Rita’s were produced during proto-interaction or embedded stages of its lifespan. Forty-seven TCTORs were produced during the first two clusters while Rita was beginning to interact with the westerlies (Figure 11(a)). Rita produced its last four clusters, including 50 TCTORs, after having tracked to the northeast and embedded in the westerlies as a short wave trough (Figure 11(b)).

#### 4. Discussion

The results of this study suggest that TCs produce more TCTORs when they begin to interact with, or are embedded within, the westerlies. One must consider that a partial reason for the abundance of TCTORs produced by proto-interaction and embedded TCs is the geographical location of the contiguous United States, which is within the mid-latitudes where the westerlies are located. Therefore, when TCs produce TCTORs in the contiguous United States, they are proximate typically to the westerlies. This is not always the case, however, because the westerly wind belt varies between zonal and meridional flow regimes and does not span continuously the same latitudes. The westerly wind belt, for example, may vary over daily and weekly time scales as trough/ridge complexes propagate or retrograde through the mid-latitudes. The westerly wind belt also tends to expand southward and strengthen with the increasing equator-to-pole temperature gradient as the North Atlantic hurricane season progresses towards fall.

As a TC tracks into the westerlies, it often undergoes internal changes in response to changes in its surrounding environment (Jones *et al.*, 2003; Wang and Wu, 2004). Certain environmental dynamic forcings that a TC may encounter, such as upper-level trough interaction and vertical wind shear, promote internal changes to the TC environment that are favourable for severe convective storms and TCTORs. TCs tracking towards and to the east of a mid-latitude trough, for example, track into an environment that is favourable for widespread convection as a result of synoptic-scale upper-level divergence. Furthermore, the

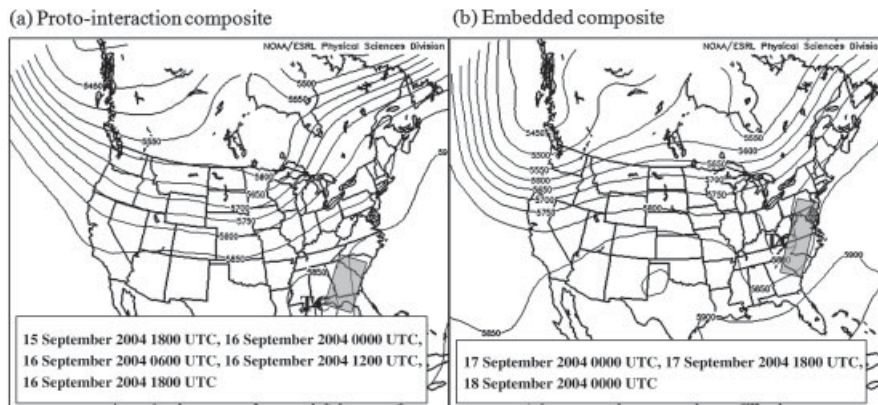


Figure 9. Composite plots of 500 hPa geopotential height (m) associated with tropical cyclone tornado (TCTOR) clusters produced by tropical cyclone (TC) Ivan (2004) when (a) beginning to interact with the westerlies and (b) when embedded within the westerlies. The grey polygon represents the general location of the clusters. Plots obtained from NOAA (2013).

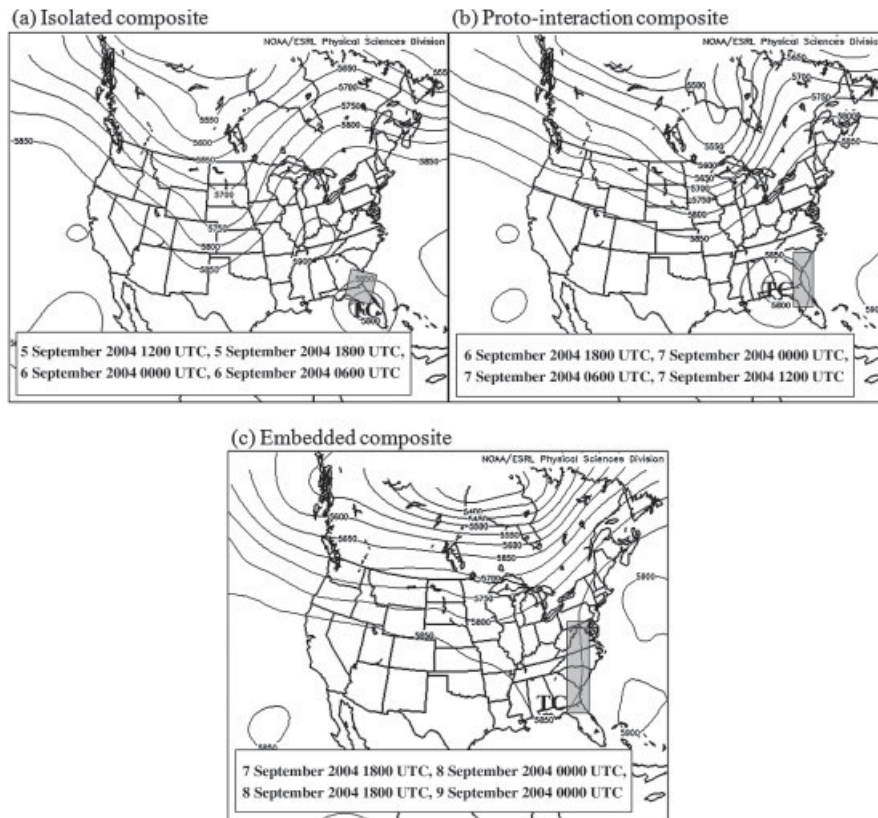


Figure 10. Composite plots of 500 hPa geopotential height (m) associated with tropical cyclone tornado (TCTOR) clusters produced by tropical cyclone (TC) Frances (2004) when (a) isolated from the westerlies, (b) when beginning to interact with the westerlies, and (c) when embedded within the westerlies. The grey polygon represents the general location of the clusters. Plots obtained from NOAA (2013).

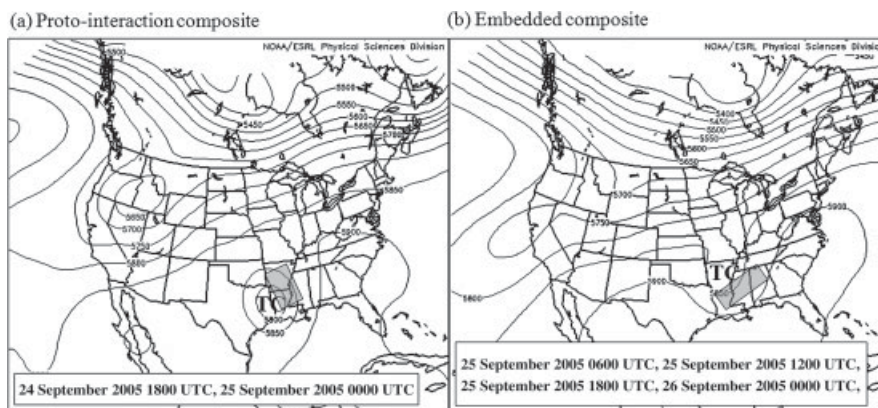


Figure 11. Composite plots of 500 hPa geopotential height (m) associated with tropical cyclone tornado (TCTOR) clusters produced by tropical cyclone (TC) Rita (2005) when (a) beginning to interact with the westerlies and (b) when embedded within the westerlies. The grey polygon represents the general location of the clusters. Plots obtained from NOAA (2013).

proximity of TCs to an upper-level jetstreak in this environment provides an additional source of rising motion (Cohen, 2010; Moore and Dixon, 2013).

The introduction of a TC into the westerlies provides an environment in which winds veer with height. Environments with veering wind profiles are favourable for supercellular storms (Davies-Jones, 1984); supercells within the TC environment are known to produce the majority of TCTORs (Edwards *et al.*, 2012). In addition, the increased vertical wind shear associated with the westerlies has been proposed to induce differential downshear vorticity advection with height across a TC, which in

turn may induce low-level convergence and cyclonically rising motion in the downshear half of the TC's environment (Frank and Ritchie, 1999, 2001). Observational studies have provided evidence in support of this proposition by showing that instability and wind shear indicators such as convective precipitation, lightning density, convective available potential energy, storm relative helicity and localized vertical wind shear are greatest in the downshear half, particularly the downshear left quadrant, of the TC environment (Corbosiero and Molinari, 2003; Molinari and Vollaro, 2008, 2010a, 2010b; Matyas, 2010; Molinari *et al.*, 2012). When located in westerly environmental shear, the

downshear half of a TC corresponds spatially to the right half of the TC environment relative to the north where an overwhelming majority of TCTORs occur. Even with northwesterly and southwesterly shear, as might be encountered with meridional mid-latitude flow, the downshear half of the TC environment roughly overlaps with the location of maximum TCTOR activity. Because of this spatial overlap, it appears plausible that westerly environmental wind shear helps prime the TC environment for TCTORs by producing conditions that are favourable for severe convective storms.

## 5. Conclusion

In this study, 500 hPa geopotential height plots that correspond to temporal clusters of tropical cyclone tornadoes (TCTORs) were analysed and classified manually. Three primary and six sub-patterns were identified. The primary patterns represent stages of interaction with the westerlies that a tropical cyclone (TC) may experience as it tracks from the tropics and subtropics to the mid-latitudes. The sub-patterns separate each primary pattern into two groups based on whether the TC exhibited closed circulation at the 500 hPa level. TCs are capable of producing temporal clusters during all stages of westerly interaction, but statistical analysis shows that TCs that are beginning to interact with, and those embedded within, the westerlies are more likely to produce more and more prolific TCTOR clusters than isolated TCs.

The results of this study suggest that the westerlies may modify the TC environment in a way that favours tornadogenesis. One possibility is that westerly vertical wind shear tilts the TC vortex downwind with increasing height, and that deep convective circulation with helically rising updrafts is initiated in the downshear quadrants of the TC environment to orient the vortex back into a vertical position (Frank and Ritchie 2001). Other instability and shear indicators such as convective precipitation, lightning density, convective available potential energy, and storm relative helicity also have been shown to be greatest in the downshear quadrants of the TC environment (Corbosiero and Molinari, 2003; Molinari and Vollaro, 2008, 2010a, 2010b; Matyas, 2010; Molinari *et al.*, 2012). The downshear region where these instability and shear indicators are greatest spatially corresponds to the region within the TC environment where TCTORs are overwhelmingly common.

Although large-scale features such as the westerlies likely play a role in priming the downshear quadrants of a TC for tornadogenesis, they are not an exclusive forcing. Other forcings, such as dry air entrainment into the TC environment and interaction with baroclinic zones, in addition to other meso- and storm-scale processes, also play a role in producing TCTOR-favourable environments (Curtis, 2004; Edwards and Pietrycha, 2006; Edwards *et al.*, 2012). In addition to other forcing, the current classification scheme can be refined further to account for additional factors such as westerly flow regime (zonal or meridional), trough tilt and amplitude, and distance between TCTOR clusters and jetstream and jetstreak axes. Continued refinement of the current classification and investigation of forcing mechanisms is needed to gain a better understanding of the environment in which TCTORs occur. Information gained through such investigation will not only provide insight into cross-scale interactions and forcings associated with TCTORs, it also will help forecasters anticipate which TCs are likely to produce a large number of TCTORs, and when in their lifespan they are most likely to produce them.

## References

- Baker AK, Parker MD, Eastin MD. 2009. Environmental ingredients for supercells and tornadoes within Hurricane Ivan. *Weather Forecast.* **24**: 223–243.
- Belanger JI, Curry JA, Hoyos CD. 2009. Variability in tornado frequency associated with U.S. landfalling tropical cyclones. *Geophys. Res. Lett.* **36**: L17805.
- Cohen AE. 2010. Synoptic-scale analysis of tornado-producing tropical cyclones along the Gulf Coast. *Natl. Weather Dig.* **34**: 99–115.
- Corbosiero KL, Molinari J. 2003. The effects of vertical wind shear on the distribution of convection in tropical cyclones. *Mon. Weather Rev.* **130**: 2110–2123.
- Curtis L. 2004. Midlevel dry intrusion as a factor in tornado outbreaks associated with landfalling tropical cyclones from the Atlantic and Gulf of Mexico. *Weather Forecast.* **19**: 411–427.
- Davies-Jones R. 1984. Streamwise vorticity: the origin of updraft rotation in supercell storms. *J. Atmos. Sci.* **41**: 2991–3006.
- Doswell CA. 1987. The distinction between large-scale and mesoscale contribution to severe convection: a case study example. *Weather Forecast.* **2**: 3–16.
- Doswell CA, Weiss SJ, Johns RH. 1993. Tornado forecasting: a review. In *The Tornado: Its Structure, Dynamics, Prediction, and Hazards*, Church C, Burgess D, Doswell C, Davies-Jones R (eds). American Geophysical Union: Washington, DC; 557–551.
- Edwards R. 2008. Tropical cyclone tornadoes - a research and forecasting overview. Part I: Climatologies, distribution, and forecast concepts. In *24th Conference on Severe Local Storms*. American Meteorological Society: Savannah, GA; 7.A.1. [http://ams.confex.com/ams/24SLS/techprogram/paper\\_141721.htm](http://ams.confex.com/ams/24SLS/techprogram/paper_141721.htm) (accessed 4 May 2011).
- Edwards R. 2010a. Tropical cyclone tornado records for the modernised NWS era. In *25th Conference on Severe Local Storms*. American Meteorological Society: Denver, CO; 3.1. [http://ams.confex.com/ams/25SLS/techprogram/paper\\_175269.htm](http://ams.confex.com/ams/25SLS/techprogram/paper_175269.htm) (accessed 4 May 2011).
- Edwards R. 2010b. *TCTOR Dataset*. <http://www.sp.noaa.gov/misc/edwards/TCTOR/tctor.xls> and <http://www.sp.noaa.gov/misc/edwards/TCTOR/readme.txt> (accessed 2 May 2011).
- Edwards R. 2012. Tropical cyclone tornadoes: a review of knowledge in research and prediction. *Electron. J. Severe Storms Meteorol.* **7**: 1–33.
- Edwards R, Dean AR, Thompson RL, Smith BT. 2012. Convective mode for significant thunderstorms in the contiguous United States. Part III: Tropical cyclone tornadoes. *Weather Forecast.* **27**: 1507–1519.
- Edwards R, Pietrycha AE. 2006. Archetypes for surface baroclinic boundaries influencing tropical cyclone tornado occurrence. In *23rd Conference on Severe Local Storms*. American Meteorological Society: St. Louis, MO; 8.2. [http://ams.confex.com/ams/23SLS/techprogram/paper\\_114992.htm](http://ams.confex.com/ams/23SLS/techprogram/paper_114992.htm) (accessed 4 May 2011).
- Frank WM, Ritchie EA. 1999. Effects of environmental flow upon tropical cyclone structure. *Mon. Weather Rev.* **127**: 2044–2061.
- Frank WM, Ritchie EA. 2001. Effects of vertical wind shear on the intensity and structure of numerically simulated hurricanes. *Mon. Weather Rev.* **129**: 2249–2269.
- Gentry RC. 1983. Genesis of tornadoes associated with hurricanes. *Mon. Weather Rev.* **111**: 1793–1805.
- Harman JR. 1991. *Synoptic Climatology of the Westerlies: Process and Patterns*. Washington, DC: Association of American Geographers.
- Hill EL, Malkin W, Schulz WA. 1966. Tornadoes associated with cyclones of tropical origin—practical features. *J. Appl. Meteorol.* **5**: 745–763.
- Johns RH, Doswell CA. 1992. Severe local storms forecasting. *Weather Forecast.* **7**: 588–612.
- Jones SC, Harr PA, Abraham J, Bosart LF, Bowyer PJ, Evans JL, Hanley DE, Hanstrum BN, Hart RE, Lalaurette F, Sinclair MR, Smith RK, Thorncroft C. 2003. The extratropical transition of tropical cyclones: forecast challenges, current understanding, and future direction. *Weather Forecast.* **18**: 1052–1092.
- McCaul EW Jr. 1991. Buoyancy and shear characteristics of hurricane-tornado environments. *Mon. Weather Rev.* **119**: 1954–1978.
- McCaul EW Jr, Weisman ML. 1996. Simulations of shallow supercell storms in landfalling hurricane environments. *Mon. Weather Rev.* **124**: 408–429.
- Matyas CJ. 2010. Locating convection in landfalling tropical cyclones: A GIS-based analysis of radar reflectivities and comparison to lightning-based observations. *Phys. Geogr.* **31**: 385–406.
- Mesinger F, DiMego G, Kalnay E, Mitchell K, Shafran PC, Ebisuzaki W, Jović D, Woollen J, Roger E, Berbery EH, Ek MB, Fan Y, Grumbine R, Higgins W, Li H, Lin Y, Manikin G, Parrish D, Shi W. 2006.

- North American Regional Reanalysis. *Bull. Am. Meteorol. Soc.* **87**: 343–360.
- Molinari J, Roms DM, Vollaro D, Nguyen L. 2012. CAPE in tropical cyclones. *J. Atmos. Sci.* **69**: 2452–2463.
- Molinari J, Vollaro D. 2008. Extreme helicity and intense convective towers in Hurricane Bonnie. *Mon. Weather Rev.* **136**: 4355–4372.
- Molinari J, Vollaro D. 2010a. Distribution of helicity, CAPE, and shear in tropical cyclones. *J. Atmos. Sci.* **67**: 274–284.
- Molinari J, Vollaro D. 2010b. Rapid intensification of a sheared tropical storm. *Mon. Weather Rev.* **138**: 3869–3885.
- Moore TW, Dixon RW. 2011. Climatology of tornadoes associated with Gulf Coast-landfalling hurricanes. *Geogr. Rev.* **101**: 371–395.
- Moore TW, Dixon RW. 2013. Preliminary analysis of the synoptic-scale environment associated with tropical cyclone tornado clusters, 1995–2010. *36th Applied Geography Conference*. Annapolis, MD. <http://applied.geog.kent.edu/AGCPapers/2013/Index2013.htm> (accessed 6 January 2013).
- NOAA. 2013. *3-Hourly NCEP North American Regional Reanalysis (NARR) Composites*. <http://www.esrl.noaa.gov/psd/cgi-bin/data/narr/plothour.pl> (accessed 1 August 2013).
- Novlan DJ, Gray WM. 1974. Hurricane-spawned tornadoes. *Mon. Weather Rev.* **102**: 476–488.
- Schultz LA, Cecil DJ. 2009. Tropical cyclone tornadoes, 1950–2007. *Mon. Weather Rev.* **137**: 3471–3484.
- Smith JS. 1965. The hurricane-tornado. *Mon. Weather Rev.* **93**: 453–459.
- Verbout SM, Schulz DM, Leslie LM, Brooks HE, Karoly DJ, Elmore KL. 2007. Tornado outbreaks associated with landfalling hurricanes in the North Atlantic basin: 1954–2004. *Meteorol. Atmos. Phys.* **97**: 255–271.
- Wang Y, Wu C-C. 2004. Current understanding of tropical cyclone structure and intensity changes – a review. *Meteorol. Atmos. Phys.* **87**: 257–278.
- Yarnal B. 1993. *Synoptic Climatology in Environmental Analysis: A Primer*. Belhaven Press: London; 256.